The American Journal of Pathology, Vol. 169, No. 5, November 2006

DOI: 10.2353/ajpath.2006.060445

Cardiovascular, Pulmonary and Renal Pathology

Teratogen-Induced, Dietary and Genetic Models of Congenital Diaphragmatic Hernia Share a Common Mechanism of Pathogenesis

Robin D. Clugston,* Jürgen Klattig,† Chistoph Englert,† Margaret Clagett-Dame,‡ Jelena Martinovic,§ Alexandra Benachi,§ and John J. Greer*

From the Department of Physiology, University of Alberta, Edmonton, Alberta, Canada; Leibniz Institute for Age Research–Fritz Lipmann Institute,† Jena, Germany; Department of Biochemistry,‡ University of Wisconsin-Madison, Madison, Wisconsin; and Hopital Necker-Enfants Malades,§ Paris, France*

Congenital diaphragmatic hernia (CDH) is a frequently occurring, major congenital abnormality that has high mortality and significant morbidity in survivors. Currently, the pathogenesis of CDH is poorly understood. In this study, we have compared the anatomical characteristics of diaphragm defects in the well-described nitrofen model with the pathogenesis of CDH in vitamin A-deficient rats and *wt1* null-mutant mice, representing teratogen-induced, dietary and genetic models of CDH, respectively. Our histological investigations, aided by three-dimensional reconstruction of the developing diaphragm, revealed a common pathogenic mechanism with regards to the location of the diaphragm defect in the foramen of Bochdalek (posterolateral diaphragm) and specific abnormalities within the primordial diaphragm. Furthermore, our analysis of postmortem specimens highlighted similarities in human cases of CDH and these animal models, supporting our hypothesis that CDH in humans arises from a defect in the primordial diaphragm. Immunohistochemical data were consistent with the defect in the primordial diaphragm being in the nonmuscular component. Importantly, these data show that very distinct models of CDH all share a common pathogenic mechanism and, together with supporting evidence from pathological specimens, highlight our proposed pathogenic model for CDH. *(Am J Pathol 2006, 169:1541–1549; DOI: 10.2353/ajpath.2006.060445)*

Congenital diaphragmatic hernia (CDH) is a severe developmental defect occurring in approximately 1 in 2500 live births and accounting for ~8% of all major congenital anomalies.[1,2] Reports of the CDH mortality rate range from 32 to 62%,[3,4] with some specialized, tertiary care centers achieving survival rates in excess of 80%.[5–7] There is significant long-term morbidity among survivors.[8–10] The majority of CDH cases (>95%) involve incomplete formation of the posterolateral portion of the diaphragm, clinically referred to as a Bochdalek hernia, most commonly occurring on the left side.[11] The hole in the diaphragm allows the abdominal viscera to invade the thoracic cavity, thereby impeding normal lung development. Lung hypoplasia and concomitant pulmonary hypertension contribute to the high mortality rate and morbidity associated with CDH.[12]

The pathogenesis and etiology of CDH are not well understood. Some insights have been derived from studies of teratogen-induced CDH in rodent models, particularly the nitrofen model. The defect in this model can be traced back to a malformation of the amuscular component of the primordial diaphragm, the pleuroperitoneal fold (PPF[13,14]). However, as Gosche[15] stressed in a recent commentary, further advances will depend on experimental data derived from additional animal models. Specifically, a case for the primary diaphragm defect being linked to a malformation of the PPF will be greatly enhanced if a common pathogenesis is discovered in distinct animal models. In this study, we take an important step in that direction by analyzing and comparing diaphragm defects in the well-characterized nitrofen model with vitamin A-deficient (VAD) rats and Wilm's Tumor 1 (*wt1*) mutant mouse models of Bochdalek CDH. Furthermore, we examined postmortem CDH diaphragm tissue to determine whether the pattern of muscularization is

Supported by the Canadian Health Institutes for Research, March of Dimes, Alberta Foundation for Medical Research.

Accepted for publication July 20, 2006.

Address reprint requests John J. Greer, Ph.D., University of Alberta, Department of Physiology, 513 HMRC, Edmonton, AB, Canada, T6G 2S2. E-mail: john.greer@ualberta.ca.

consistent with the proposed pathogenic mechanism discovered in animal models.

Diaphragm defects in VAD rats were initially observed over 50 years ago.[16–18] Furthermore, data from the teratogenic CDH models provided evidence for a role of retinoid signaling in the etiology of CDH (reviewed by Greer[19]). In this study, we used a modified VAD paradigm[20] to examine the pathogenesis of the diaphragm defect in this model of CDH.

The past 10 years have seen several reports of diaphragm defects in genetically engineered mutant mice, introducing potential genetic models for the study of this disease and further insight into its genetic etiology. Bochdalek diaphragmatic hernias have been observed in Wilms' Tumor 1 (*wt1*) null-mutant mice, retinoic acid receptor (*RAR*) α and *RARβ2* double null-mutant mice, *MyoR* and *Capsulin* double null-mutant mice, and most recently in mice with *COUP-TFII* conditionally inactivated in *Nkx3-2*-expressing tissues.[21–24] *Wt1* null-mutant mice were originally created to study the role of *wt1* in urogenital development, diaphragm defects being only an incidental observation.[21] The *WT1* gene, mutated in 10 to 15% cases of human Wilms' Tumor, encodes a DNA-binding protein with four zinc fingers and is thought to function as a transcription factor, as well as having a role in RNA processing.[25] We chose to focus on *wt1* null-mutant mice in this study because it is expressed in the developing PPF of humans (Pritchard-Jones et al[26]; see Figure 2i) and because there have been several descriptions of congenital syndromes in humans that include CDH within their spectrum of abnormalities and have their origins in *WT1* mutations. These syndromes include Denys-Drash syndrome, Wilms tumor aniridia growth retardation syndrome, and Meacham syndrome.[27–29]

We hypothesized that the anatomical hallmarks of the teratogenic, VAD, and *wt1* models are the same; specifically, that the diaphragm defects are 1) in the foramen of Bochdalek, 2) can be traced back to abnormalities in the PPF, and 3) are consistent with initial defects arising in the amuscular component of the PPF.

Materials and Methods

Nitrofen Treatment

Timed pregnant animals were used for all experiments in accordance with guidelines established by the Animal Welfare Committee at the University of Alberta. Noon of the day on which a sperm plug was observed in the breeding cage was determined as embryonic day (E)0.5. Nitrofen was obtained from the China National Construction Jiangsu Company (Nanjing, China). Timed pregnant Sprague-Dawley rats were treated with nitrofen at noon E8. One hundred mg of nitrofen was dissolved using a sonicator (Trans-sonic 310; Elma Singen, Germany) in 1 ml of olive oil; this mixture was then fed to lightly anesthetized (2% halothane, balance 95% O_2 and 5% CO_2) dams by gavage.

Vitamin A-Deficient Rats

A full description of the technique to render animals VAD has been previously described.[30] In brief, weanling female rats (Harlan-Sprague-Dawley) were fed a special diet devoid of all forms of vitamin A to render them VAD and were subsequently recovered on a limiting amount of all-*trans* retinoic acid (atRA; 12 μg/g diet) before mating. Pregnant rats from all groups received 12 μg/g diet atRA starting at E0.5 until day E8.5. Animals in the first control group continued on a diet of 12 μg/g diet atRA, which was supplemented with 100 units/day of retinyl palmitate after E8.5. A second group of control animals received 250 μg/g diet atRA between E8.5 and E10.5 and were then transferred to a diet containing a combination of atRA and retinyl palmitate (12 μg/g diet and 100 units/day, respectively). VAD animals also received 250 μg/g diet atRA between E8.5 and E10.5 but then received only a 12-μg atRA/g diet. Note that E8.5 to E10.5 represents a critical period during rat gestation that requires a high dose of dietary atRA to support later embryonic survival (Ref. 20). A complete description of this late embryonic VAD model will be presented elsewhere (A.W.-M. See and M. Clagett-Dame, in preparation).

Wt1 Null-Mutant Mice

Wt1 was functionally knocked out by the insertion of the *neo*-resistance cassette into the first exon of the gene on a C57BL/6 mouse background; a full description of how these mice were generated has previously been published.[21] In these experiments, we used animals from a mixed MF1 $\times$ C57BL/6 background.[31]

Caesarian Section and Tissue Preparation

At the desired gestational age, animals were anesthetized with halothane ($\sim$3% delivered in 95% O_2 and 5% CO_2) or ether and caesarian sections performed to remove the fetal tissue. Gestational ages of isolated fetuses were confirmed by measurement of crown-rump length.[32] Isolated fetuses were decapitated and the hindquarters removed, and the remaining trunk of the fetus was fixed by immersion in 4% paraformaldehyde for at least 24 hours at 4°C.

Diaphragm Wholemounts

A dissecting microscope (Leica Wild M3C; Wetzlar, Germany) was used to isolate whole diaphragms from fixed fetal rodent tissue, which were then rinsed in phosphate-buffered saline (PBS). Digital photographs of free-floating diaphragms were taken using a Nikon 990 digital camera (Nikon, Tokyo, Japan).

Diaphragm and Whole Embryo Histology

Isolated diaphragms and embryos were dehydrated in a graded series of alcohol and embedded in paraffin wax. Transverse sections were cut at 10 μm on a rotary

microtome (Leica RM2135) and mounted on presubbed glass slides. The slides were counterstained with hematoxylin and eosin, dehydrated in ethanol, and coverslipped.

Three-Dimensional Modeling

A complete series of consecutive sections spanning the rostral to caudal extent of the PPF were digitally photographed. Each section was 10 μm and was prepared in the same way as described in the histology section. Three-dimensional (3-D) models were created using Rhinoceros-3D modeling software (Seattle, WA). A curve outlining the PPF was made from each image; these curves were then collated to create a wire frame model of the PPF to which a surface was digitally added, thus creating an accurate 3-D rendering of the PPF. For clarity, the esophageal mesentery was excluded when outlines of the PPF were being generated.

Immunohistochemistry

We examined the expression of wt1, COUP-TFII, and Pax3 within the PPF of rats at age E13.5. Experiments were repeated in triplicate to confirm the patterning of staining. Double-labeling experiments using antibodies for wt1 (monoclonal mouse anti-human, M3561, 1:50 dilution; Dako Canada, Mississauga, ON, Canada), COUP-TFII (monoclonal mouse anti-human, H7147; 1:250 dilution; PPMX Perseus Proteomics Inc., Tokyo, Japan), and Pax3 (goat polyclonal anti-human, sc-7748, 1:100 dilution; Santa Cruz Biotechnology, Santa Cruz, CA) were performed on 10-μm-thick paraffin-embedded sections mounted on glass slides according to the following protocol. Sections were dewaxed in xylene and then rehydrated using a graded series of alcohol. Sections were rinsed in PBS, microwaved in 0.01 mol/L sodium citrate buffer, pH 6, at 600 W for 5 minutes, and then pretreated with 1% hydrogen peroxide in 100% methanol for 30 minutes. Sections were treated with 1% bovine serum albumin (Sigma, St. Louis, MO) in 0.4% Triton X-100/PBS for 30 minutes before incubation with the appropriate primary antibody. All primary antibodies were diluted in PBS with 0.1% bovine serum albumin and 0.4% Triton X-100; the antibodies were left to incubate overnight at room temperature. After incubation with primary antibodies, the sections were washed with PBS and incubated with a mixture of fluorophore-conjugated secondary antibodies diluted in PBS and 0.1% bovine serum albumin for 2 hours. For wt1 and Pax3 double labeling, Cy3-conjugated donkey anti-mouse (1:200; Jackson ImmunoResearch, West Grove, PA) and Cy5-conjugated donkey anti-goat (1:200; Jackson ImmunoResearch) secondary antibodies were used, respectively. COUP-TFII and Pax3 double labeling was performed using Cy3-conjugated donkey anti-mouse (1:200) and Cy5-conjugated donkey anti-goat (1:200) secondary antibodies, respectively. After 2 hours, sections were further washed in PBS and coverslipped with Fluorsave mounting medium (Calbiochem, San Diego, CA).

Wt1 and COUP-TFII double labeling was performed using the tyramide signal amplification kit protocol (PerkinElmer Life Sciences, Boston, MA). In brief, sections were pretreated in 3% H_2O_2 in PBS, washed in TNT buffer (0.1 mol/L Tris-HCl, pH 7.5, 0.15 mol/L NaCl, and 0.05% Tween 20), and incubated in TNB-T (0.1 mol/L Tris-HCl, pH 7.5, 0.15 mol/L NaCl, 0.5% bovine serum albumin, and 0.3% Triton X-100). Sections were incubated with the wt1 antibody diluted 1:4000 in TNB-T overnight. After several washes in TNT, sections were incubated for 2 hours in biotinylated donkey anti-rabbit (1:200). Biotin was revealed using the tyramide signal amplification kit. Sections were incubated with streptavidin-horseradish peroxidase (1:150) for 30 minutes followed by tyramide conjugated to fluorescein (1:75), diluted in amplification diluent, for 10 minutes. After wt1 labeling, sections were extensively washed in TNT and incubated for 30 minutes in TNB-T followed by anti-COUP-TFII antibody (1:250) in TNB-T overnight. The following day, sections were incubated with donkey anti-rabbit-Cy3 (1:200) in TNB for 2 hours, washed, mounted on slides, and coverslipped with Fluorsave solution.

Confocal Microscopy

Immunostained sections were scanned with a Zeiss Axioplan microscope ($\times$20 objective) using an LSM 510 NLO laser configured to a computer running LSM 510 software (Zeiss, Jena, Germany). For Cy3 fluorescence, excitation (HeNe, 1 mV) was set to 543 nm, and emissions were collected using a 560-nm long-pass filter. For Cy5 fluorescence, excitation (HeNe, 1 mV) was set to 633 nm, and emissions were collected using a 630-nm long-pass filter. Acquired images were exported in bitmap format and prepared for publication in Adobe Photoshop 6.0 (Adobe Systems, Mountains View, CA).

Human Tissue

In accordance with French law, institutional ethics policy, and parental consent for unrestricted autopsy and genetic testing, postmortem diaphragmatic tissues from human cases of CDH, obtained by the Department of Embryo-Fetopathology, Hopital Necker-Enfants Malades (Paris, France) were removed at autopsy and fixed in 10% phosphate-buffered formalin before further examination.

Statistical Methods

Numerical results are expressed as means $\pm$ the SD. Diaphragm thickness data were tested using a paired Student's *t*-test; differences were considered significant at P values <0.05.

Results

Characterization of Diaphragm Defects

The first stage of the study was to characterize the defects in the diaphragm of the various CDH rodent

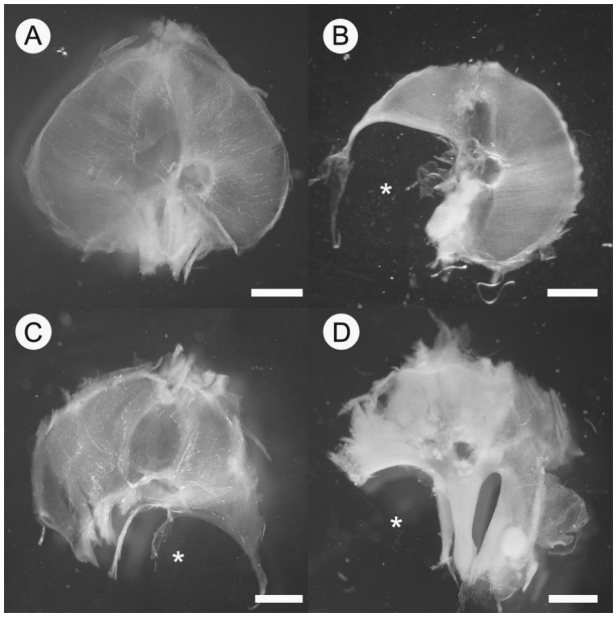

Figure 1. Photomicrographs of whole diaphragms isolated from control (**A**), nitrofen-treated rat (**B**), VAD rat (**C**), and *wt1* null-mutant mouse (**D**), showing representative examples of Bochdalek diaphragm defects (*). Diaphragms are oriented such that the top of the image is anterior and the bottom of the image is posterior. Scale bar = 2 mm.

models. E16.5 fetuses removed from nitrofen-treated rats, VAD rats, and *wt1* null-mutant mice were used to study the whole diaphragm. These animals all appeared grossly normal compared with control embryos. Dissection of the thoracic cavity revealed hypoplastic lungs and abdominal contents protruding into the cavity through a hole in the diaphragm (data not shown). Figure 1 illustrates a representative selection of diaphragm defects observed, all of which were positioned posterolaterally, in the foramen of Bochdalek. No diaphragm defects were observed in control animals. Treatment with 100 mg of nitrofen on E8 yielded posterolateral diaphragm defects in ~50% of offspring, the majority of which were on the left side; this was consistent with previously published data.[13] Diaphragm defects were observed in all of the VAD fetuses examined (n = 5), and the majority of the diaphragm defects were on the right side or were bilateral, ie, holes in the left and right posterolateral portion of the diaphragm. Left-sided posterolateral defects were also observed in *wt1* null-mutant tissue (n = 3); however, due to the small number of fetuses examined, an accurate incidence of diaphragmatic hernia in these mice could not be calculated, although it should be noted that not every *wt1* null-mutant fetus had a diaphragm defect.

The characterization of the defects in rodent models of CDH was complemented by examination of human diaphragms collected at autopsy from fetuses of varying gestational age. A normally developed diaphragm at 35 weeks of gestation is shown for comparison with a diaphragm isolated from a fetus at 34 weeks of gestation with a large left-sided diaphragm defect; another dia-

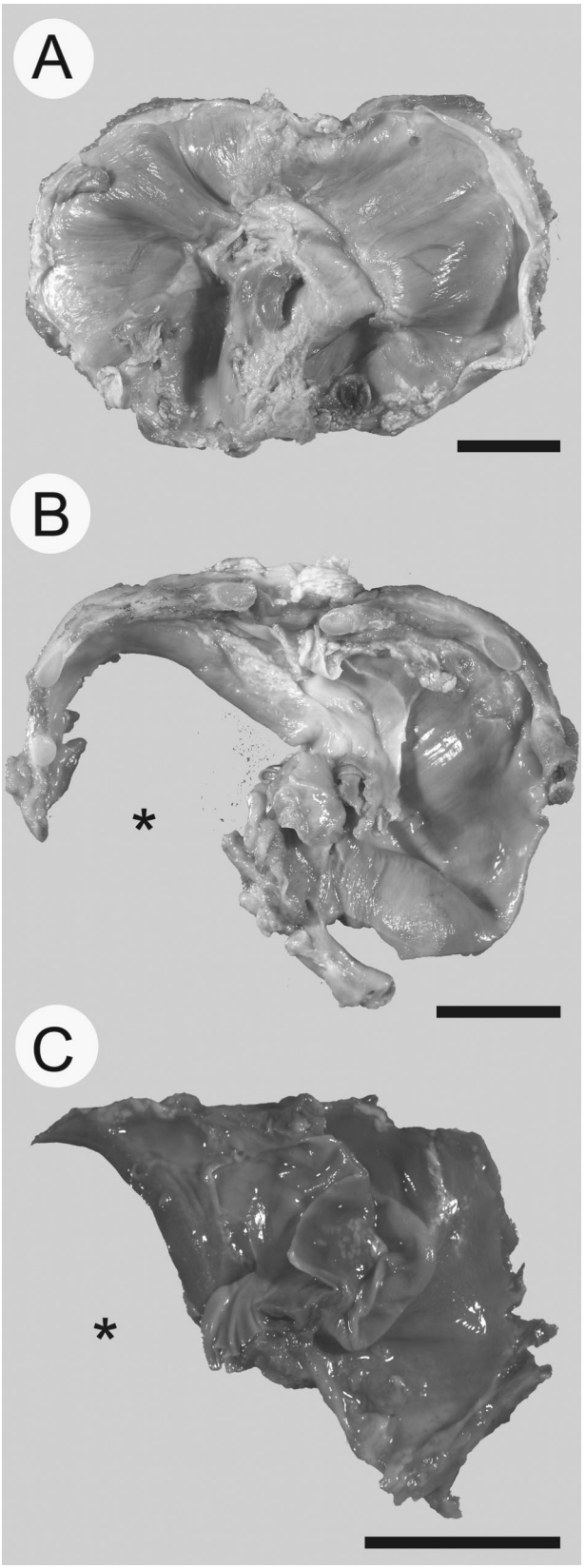

Figure 2. Photomicrographs of human diaphragms. A normal diaphragm at 35 weeks of gestation (**A**) is shown for comparison against a diaphragm isolated from a fetus at 34 weeks of gestation (**B**) with a large left-sided diaphragm defect (*) and a diaphragm isolated from a 30-week fetus (**C**) also with a left-sided defect (*). Diaphragms are oriented such that the top of the image is anterior and the bottom of the image is posterior. Scale bar = 2 cm.

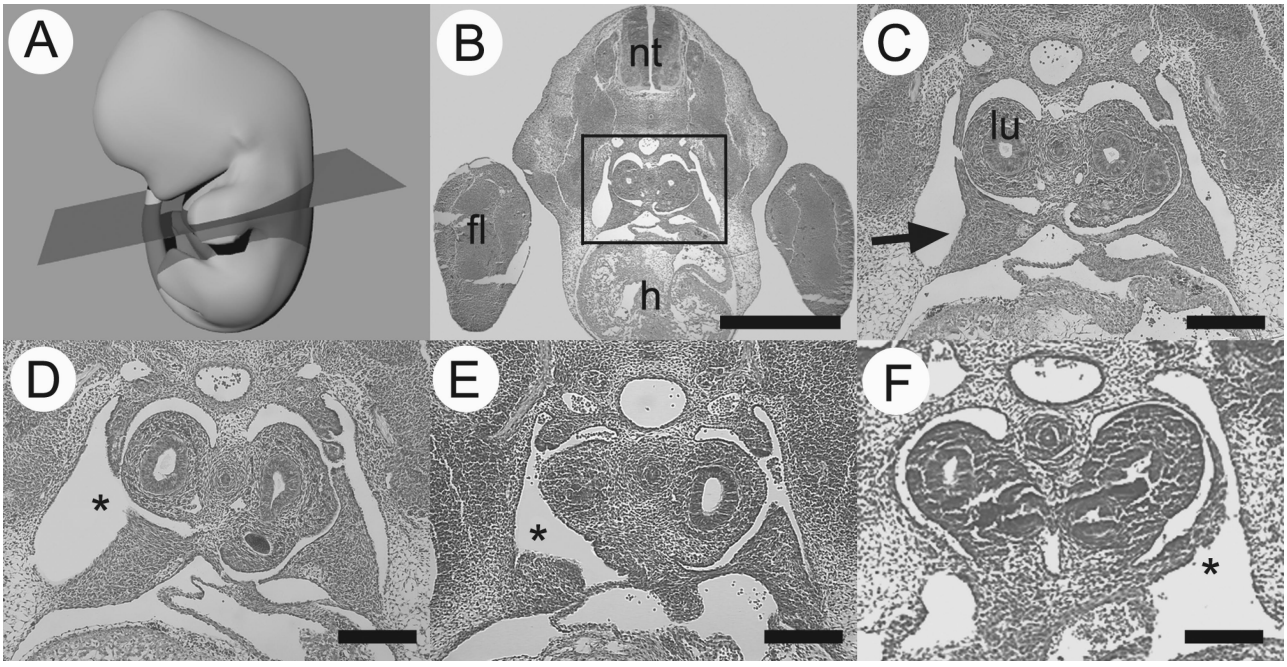

Figure 3. Diaphragm defects have their origin in an abnormal PPF. A schematic representation of an E13.5 rat is provided with the plane of section shown to orient the reader (**A**). A transverse section through the cervical region of an E13.5 rat embryo (**B**) shows the neural tube (nt), forelimb (fl), and heart (h). The boxed region, when viewed at higher power (**C**), contains the developing lungs (lu) and the triangular PPFs (**arrow**). Representative PPF defects (*) are shown from nitrofen-treated (**D**), VAD (**E**), and *wt1* null-mutant (**F**) animals. Scale bar in **B** = 1 mm, scale bar in **C–F** = 200 μm.

phragm with a large left-sided defect is also shown after 30 weeks of gestation (Figure 2).

Characterization of PPF Defects

The next stage of the study was to examine the defects in the primordial diaphragm (PPF) in each of the rodent CDH models. Embryos from control, nitrofen-treated, and VAD rats were collected at E13.5, and *wt1* null-mutant mouse tissue was collected at E12.5 of gestation. Transverse sections were cut through the embryos at a cervical level to examine the PPF as shown in Figure 3. The PPFs in control animals were triangular-shaped structures protruding out from the lateral body wall. Consistent with original reports by Allan and Greer,[13] nitrofen-treated animals commonly had an abnormal PPF structure, characterized by the absence of the dorsally projecting point of the triangular PPF. A similar abnormality was found in the PPFs of the VAD rat embryos we examined (n = 6). Abnormal PPF structure was also seen in transverse sections of *wt1* null-mutant mice (n = 3), although the defect extended to the more lateral aspect of the PPF.

3-D reconstructions of the PPFs from control, nitrofen-treated, VAD, and *wt1* null-mutant tissue were made from serial sections of tissue cut along the rostrocaudal extent of this structure and are presented in Figure 4. Recreated in 3-D, the PPFs normally look like a pair of triangular wedge-shaped tissues joined together at their apices. The recreated PPFs from nitrofen-treated rats look similar; however, on one side there is an area of tissue missing from the posterior and caudal-most region of the PPF. Recreation of the PPF from VAD tissue yields an almost identical picture, revealing an area of tissue missing along the posterior and most caudal aspect of the PPF. Reconstruction of the PPFs in wild-type mice looks essentially identical to that of control rat tissue (data not shown). The structure of the PPFs from *wt1* null-mutant mice shows that the caudal and more anterior aspect of the PPF is unilaterally missing.

Characterization of Muscle Architecture in Defective Diaphragms

A current model of how the dorsolaterally located PPF defect translates into the characteristic hole in the dorsolateral diaphragm states that muscle precursors normally destined for the defective region accumulate on the remaining surrounding PPF mesenchyme (reviewed by Greer et al[33]). This, in turn, is subsequently manifest as a thickening of muscle adjacent to the herniated region of the diaphragm. To determine whether this was a common feature in the three rodent models and in human CDH, whole diaphragms were sectioned along their anteroposterior axis to study diaphragm thickness. As previously observed,[13] diaphragms isolated from nitrofen-treated rats were thickened around the periphery of the defect compared with the intact contralateral side (Figure 5A). Diaphragms isolated from VAD rats (n = 6) also showed a similar thickening around the defect (Figure 5B). Sufficient mature diaphragm was unavailable to draw any conclusions regarding diaphragm thickening in *wt1* null-mutant mice.

A representative example of a cross-section through a human diaphragm is shown in Figure 5C. The study of one postmortem diaphragm available to us from a non-

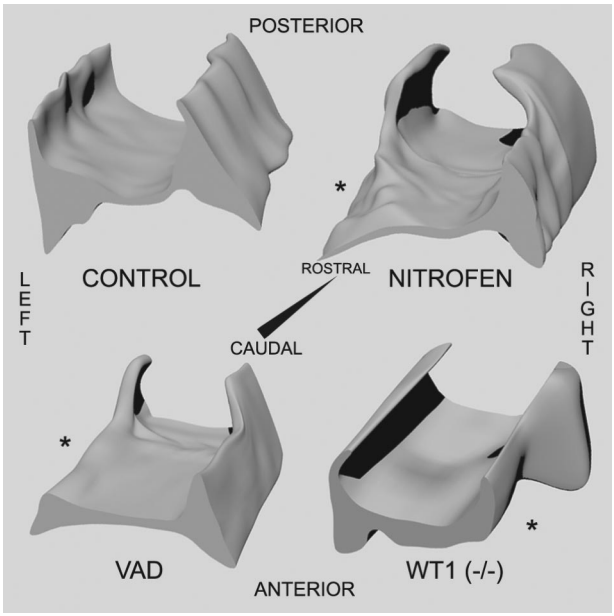

Figure 4. Three-dimensional reconstruction of PPFs recreated from control (upper left), nitrofen-treated (upper right), VAD (lower left), and *wt1* null-mutant (lower right) tissue sections. PPF defects are highlighted by an **asterisk**.

CDH case indicated that the control side of the diaphragm in cases of CDH is representative of normal diaphragm thickness. The thickness of four human diaphragms with diaphragmatic hernia was measured, and the data are presented in Figure 6 relative to the normal, contralateral side of the diaphragm. Thickness of the normal side of the diaphragm was normalized to 100%; of the four diaphragms examined, the thickness of the defective side was 183 ± 37.2%, with this change representing a significant increase in diaphragm thickness surrounding the diaphragm defect.

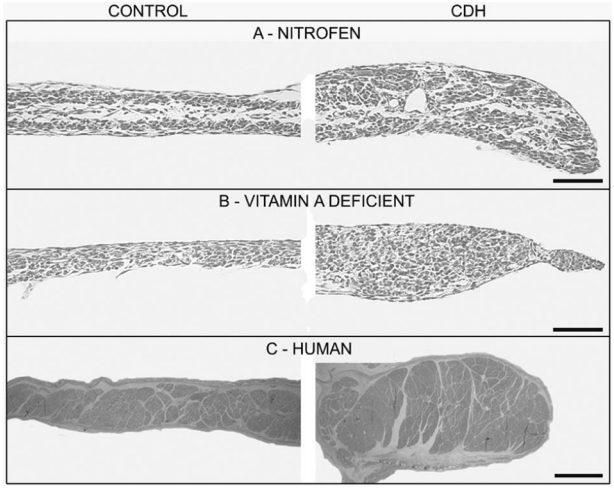

Figure 5. Diaphragm thickening is a hallmark of CDH. The musculature of the diaphragm is thicker around the diaphragm defect (right column) compared with the normal contralateral side of the diaphragm (left column) in nitrofen-exposed animals (**A**), VAD animals (**B**), and in human cases of CDH (**C**). Scale bars in **A** and **B** = 100 μmol/L; in **C**, scale bar = 2 mm.

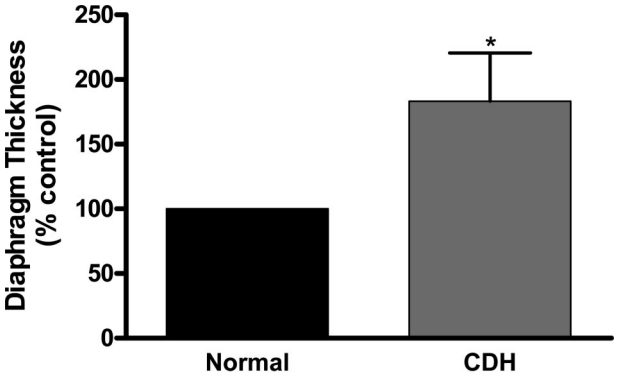

Figure 6. Graph comparing the relative thickness of the normal hemi-diaphragm and the thickness around the periphery of the defect from infants with CDH. Error bars indicate the SD of measurements from four separate diaphragms. $^*P < 0.05$, paired sample *t*-test.

Expression of wt1 and COUP-TFII in the PPF

The proposed model of the PPF defect states that the pathogenesis can be traced to a malformation of the mesenchymal tissue rather than the myogenic component of the primordial diaphragm.[33] Thus, we tested the hypothesis that wt1 protein is expressed in the nonmuscular component of the PPF. Furthermore, given that *COUP-TFII*-null mice have abnormal PPF structure and Bochdalek hernias,[24] we tested the hypothesis that COUP-TFII protein would also be expressed in nonmuscular cells of the PPF. Figure 7A demonstrates that wt1 immunopositive cells are found throughout the PPF at E13.5 of rat gestation, but there is no colocalization with Pax3, a marker of myogenic cells in the PPF.[34] Likewise, COUP-TFII is expressed in the PPF but not by Pax3-expressing myogenic cells (Figure 7B). Double immunolabeling for COUP-TFII and wt1 shows that these two proteins colocalize within the cells of the PPF, although there is not 100% overlap of expression (Figure 7C).

Discussion

In recent years, significant advances have been made in the treatment of CDH; however, its incidence remains unchanged, and it is still unclear how and why the diaphragm defect arises, necessitating continuing research. We have demonstrated that, in addition to nitrofen treatment, vitamin A deficiency and inactivation of the *wt1* gene all result in the formation of Bochdalek-type diaphragmatic hernia, and, therefore, they can be collectively used as teratogenic, dietary and genetic models of CDH, respectively. Furthermore, examination of postmortem CDH diaphragm tissue revealed parallels between the rodent models and CDH in humans.

Nitrofen-exposed, VAD, and *wt1* null-mutant rodents all have posterolateral diaphragm defects similar in phenotype to diaphragm defects observed in infants with CDH. One of the first theories put forth to explain the pathogenesis of CDH stated that failure of the pleuroperitoneal canals to close properly allowed persistent communication between the pleural and abdominal cavities, causing the abdominal viscera to herniate into the

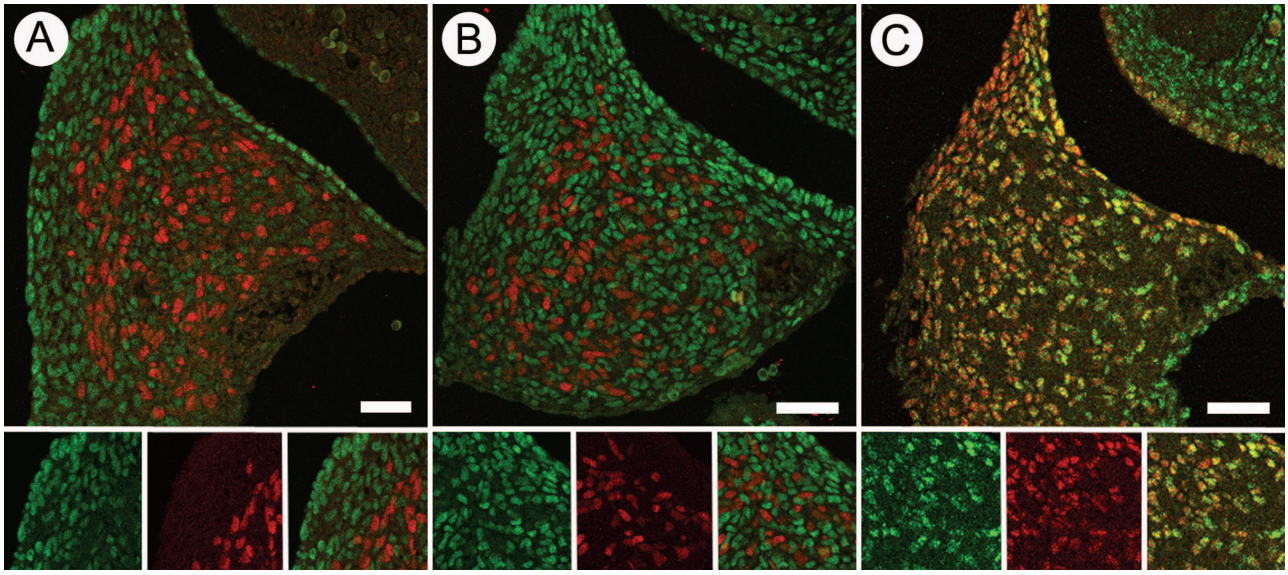

Figure 7. Representative immunohistochemical staining within the developing PPF of rats at E13.5 at ×20 magnification. **A:** Double labeling for wt1 (green) and Pax3 (red). **B:** Double labeling for COUP-TFII (green) and Pax3 (red). **C:** Double labeling for wt1 (red) and COUP-TFII (green). Double-labeled cells appear yellow. Lower panels in **A**, **B**, and **C** show the red channel, green channel, and merged images from left to right, respectively. Scale bars = 100 μm.

chest. This hypothesis was formulated on the basis of pathological specimens from infants with CDH and the study of normal diaphragm development in the embryo[35,36]; it has persisted in the literature despite the absence of supporting experimental evidence. In contrast, previous work in the nitrofen model has shown that the diaphragm defects in this model are distinct from, and occur before, pleuro-peritoneal canal closure and that a malformed PPF is the origin of the defect.[13] Here we tested the hypothesis that CDH in VAD rats and *wt1* null-mutant mice is also caused by an abnormally formed PPF, independent of pleuro-peritoneal canal closure.

In cross-section, the PPFs appear as paired, triangular-shaped structures protruding out from the lateral body wall. As previously described,[13] nitrofen treatment leads to a characteristic defect in the PPF; partial loss of PPF tissue maintains communication between the abdominal and pleural cavities and forms the basis for a hole in the developing diaphragm. VAD produces an abnormal PPF that is almost identical in appearance to the defect produced by nitrofen treatment. *WT1* null-mutant mice also have a malformed PPF. To better visualize the PPF malformations, 3-D reconstructions of the developing PPFs were made. Seen in 3-D, the paired PPFs appear as a wedge-shaped structures linked at their apex and tapering off caudally. The posteriorly projecting "base" of these wedges is absent in nitrofen-treated and VAD rats. The extent of the missing tissue in *wt1* null-mutant mice is slightly different, which may represent a subtle species difference in this stage of diaphragm development or a result of the specific mutation. Analysis of the PPF in other mutant mouse models of CDH will clarify this issue. Nevertheless, a malformed PPF underlies diaphragmatic hernia in nitrofen-treated and VAD rats and *wt1* null-mutant mice, demonstrating that three distinct models of CDH have a common pathogenic origin.

The original description of the *wt1* null-mutant phenotype described incomplete diaphragm formation and showed lung tissue herniating into the abdominal cavity.[21] In the fetuses we examined, we observed a more classic picture of CDH, with abdominal contents herniating into the pleural cavity. It seems likely that variability in the penetrance of specific abnormalities may explain this difference; pericardial bleeding and a smaller pleural cavity may raise intrathoracic pressure to a point at which it is greater than intra-abdominal pressure, pushing the lungs downwards and through the hole in the diaphragm. This phenotype was not as prevalent in the mice we examined; thus, as is typically the case in CDH, abdominal pressure was greater than thoracic pressure, and the abdominal viscera were pushed into the thoracic cavity. As detailed in the Introduction, there are several strains of mutant mice with posterolateral diaphragm defects. Our examination of *wt1* null-mutant mice provides a detailed description of the pathogenesis of diaphragm defects occurring in a genetic model of Bochdalek CDH. Genetic models for the less common subtypes of diaphragmatic hernia have also been characterized. For example, a mutation in *Fog2* produces mice with eventration of the diaphragm, and mice lacking *Slit3* expression have diaphragmatic central tendon defects, another rare form of CDH.[37–39]

Although it was not possible to study the developing PPF in human cases of CDH, phenotypic similarities between abnormal human and rodent diaphragms support the hypothesis that CDH in humans arises from an abnormal PPF. In addition to the location of the hole in the diaphragm, we demonstrated that the diaphragm is thicker around the defect in nitrofen-treated and VAD rats and that this is also a feature of diaphragms isolated from infants with CDH. We interpret thickening of the diaphragm around the defect as being caused by the ag-

gregation of muscle precursor cells that would normally spread out to populate the entire diaphragm. Accordingly, muscle precursors migrating to a malformed PPF from the somites accumulate in the remaining PPF tissue, and their subsequent proliferation and differentiation in a restricted space leads to thickening of the diaphragmatic musculature. As such, the thickening around the diaphragm defect in humans is consistent with its origins in a malformed PPF. We examined pathological diaphragm specimens, which may have produced a bias in our sample toward larger defects (and therefore thickening) since infants with CDH with large defects are more likely to die. However, diaphragm thickness, which can be measured by magnetic resonance imaging, is also increased in infants who survive the perinatal period (Dr. R. Bhargava, personal correspondence).

We could not measure diaphragm thickness in *wt1* null-mutant mice because of the lethality of the mutation. The creation of a conditional *wt1* null-mutant mouse might allow improved survival during late gestation, allowing diaphragm thickness to be directly measured; such a strain of mice would also allow the time period during which *wt1* is essential for diaphragm development to be assessed. Although diaphragm thickness was not directly measured, the conditional *COUP-TFII* knockout model of CDH appears to have a thickened diaphragm around the periphery of the defect (see You et al[24]; Figure 4C). In summary, thickening of the diaphragmatic musculature around the defect in rodent models of CDH is also a feature of CDH in humans and is indicative of an earlier defect in the PPF.

In addition to the assertion that failure of pleuro-peritoneal canal closure leads to CDH, it has also been proposed that CDH arises from an abnormality in the developing muscle of the diaphragm.[40] However, exposure of *c-met* null-mutant mice, which have an amuscular diaphragm, to nitrofen and other CDH-inducing teratogens causes diaphragm defects independent of myogenesis, supporting the hypothesis that CDH arises from an abnormality in the nonmuscular, mesenchymal substratum of the developing diaphragm.[14] Our immunohistochemical analysis of the PPF demonstrates that *wt1* and *COUP-TFII*, two genes that cause CDH when inactivated, are expressed throughout the PPF, but they are not expressed in Pax3-positive muscle precursor cells. This result indicates that it is the nonmuscle cells of the PPF that are affected in these strains of mice, supporting the hypothesis that CDH arises from a defect in the nonmuscular component of the PPF. Furthermore, wt1 and COUP-TFII double labeling suggests that these proteins colocalize within the PPF, highlighting the possibility that the same cells are being affected in both strains of mutant mice.

In summary, we have highlighted a common pathogenic mechanism in nitrofen-treated rats, VAD rats, and *wt1* null-mutant mice—representing distinct teratogenic, dietary, and genetic models of CDH respectively. Anatomical similarities between these rodent models and human tissue support the hypothesis that CDH in humans arises from a defect in the developing PPF. Furthermore, the immunohistochemical data highlight the concept that it is the nonmuscular, mesenchymal substratum of the PPF that is malformed. Future studies using a combination of the differing animal models will hopefully provide unique mechanistic insights into the etiology of CDH.

Acknowledgments

We thank Silvia Pagliardini for assistance with confocal microscopy and Jan Kowalczeski for valuable assistance in making the 3-D reconstructions of the PPF.

References

1. Tonks A, Wyldes M, Somerset DA, Dent K, Abhyankar A, Bagchi I, Lander A, Roberts E, Kilby MD: Congenital malformations of the diaphragm: findings of the West Midlands Congenital Anomaly Register 1995 to 2000. Prenat Diagn 2004, 24:596–604
2. Doyle NM, Lally KP: The CDH Study Group and advances in the clinical care of the patient with congenital diaphragmatic hernia. Semin Perinatol 2004, 28:174–184
3. Stege G, Fenton A, Jaffray B: Nihilism in the 1990s: the true mortality of congenital diaphragmatic hernia. Pediatrics 2003, 112:532–535
4. Lally KP, Lally PA, Meurs KP, Bohn DJ, Davis CF, Rodgers B, Bhatia J, Dudell G: Treatment evolution in high risk congenital diaphragmatic hernia: ten years experience. Ann Surg 2006, (in press)
5. Bagolan P, Casaccia G, Crescenzi F, Nahom A, Trucchi A, Giorlandino C: Impact of a current treatment protocol on outcome of high-risk congenital diaphragmatic hernia. J Pediatr Surg 2004, 39:313–318; discussion 313–3138
6. Al-Shanafey S, Giacomantonio M, Henteleff H: Congenital diaphragmatic hernia: experience without extracoporeal membrane oxygenation. Pediatr Surg Int 2002, 18:28–31
7. Downard CD, Jaksic T, Garza JJ, Dzakovic A, Nemes L, Jennings RW, Wilson JM: Analysis of an improved survival rate for congenital diaphragmatic hernia. J Pediatr Surg 2003, 38:729–32
8. Trachsel D, Selvadurai H, Bohn D, Langer JC, Coates AL: Long-term pulmonary morbidity in survivors of congenital diaphragmatic hernia. Pediatr Pulmonol 2005, 39:433–439
9. Poley MJ, Stolk EA, Tibboel D, Molenaar JC, Busschbach JJ: Short term and long term health related quality of life after congenital anorectal malformations and congenital diaphragmatic hernia. Arch Dis Child 2004, 89:836–841
10. Muratore CS, Kharasch V, Lund DP, Sheils C, Friedman S, Brown C, Utter S, Jaksic T, Wilson JM: Pulmonary morbidity in 100 survivors of congenital diaphragmatic hernia monitored in a multidisciplinary clinic. J Pediatr Surg 2001, 36:133–140
11. Torfs CP, Curry CJ, Bateson TF, Honore LH: A population-based study of congenital diaphragmatic hernia. Teratology 1992, 46:555–565
12. Harrison MR, Adzick NS, Estes JM, Howell LJ: A prospective study of the outcome for fetuses with diaphragmatic hernia. JAMA 1994, 271:382–384
13. Allan DW, Greer JJ: Pathogenesis of nitrofen-induced congenital diaphragmatic hernia in fetal rats. J Appl Physiol 1997, 83:338–347
14. Babiuk RP, Greer JJ: Diaphragm defects occur in a CDH hernia model independently of myogenesis and lung formation. Am J Physiol 2002, 283:L1310–L1314
15. Gosche JR, Islam S, Boulanger SC: Congenital diaphragmatic hernia: searching for answers. Am J Surg 2005, 190:324–332
16. Andersen DH: Incidence of congenital diaphragmatic hernia in the young of rats bred on a diet deficient in vitamin A. Am J Dis Child 1941, 62:888
17. Andersen DH: Effect of diet during pregnancy upon the incidence of congenital diaphragmatic hernia in the rat. Am J Path 1948, 15:163–185
18. Warkany J, Roth CB: Congenital malformations induced in rats by maternal vitamin A deficiency. J Nutr 1948, 35:1–11
19. Greer JJ, Babiuk RP, Thebaud B: Etiology of congenital diaphragmatic hernia: the retinoid hypothesis. Pediatr Res 2003, 53:726–730

20. White JC, Highland M, Clagett-Dame M: Abnormal development of the sinuatrial venous valve and posterior hindbrain may contribute to late fetal resorption of vitamin A-deficient rat embryos. Teratology 2000, 62:374–384
21. Kreidberg JA, Sariola H, Loring JM, Maeda M, Pelletier J, Housman D, Jaenisch R: WT-1 is required for early kidney development. Cell 1993, 74:679–691
22. Mendelsohn C, Lohnes D, Decimo D, Lufkin T, LeMeur M, Chambon P, Mark M: Function of the retinoic acid receptors (RARs) during development (II). Multiple abnormalities at various stages of organogenesis in RAR double mutants. Development 1994, 120:2749–2771
23. Lu JR, Bassel-Duby R, Hawkins A, Chang P, Valdez R, Wu H, Gan L, Shelton JM, Richardson JA, Olson EN: Control of facial muscle development by MyoR and capsulin. Science 2002, 298:2378–2381
24. You LR, Takamoto N, Yu CT, Tanaka T, Kodama T, Demayo FJ, Tsai SY, Tsai MJ: Mouse lacking COUP-TFII as an animal model of Bochdalek-type congenital diaphragmatic hernia. Proc Natl Acad Sci USA 2005, 102:16351–16356
25. Brown KW, Malik KT: The molecular biology of Wilms tumour. Expert Rev Mol Med 2001, 2001:1–16
26. Pritchard-Jones K, Fleming S, Davidson D, Bickmore W, Porteous D, Gosden C, Bard J, Buckler A, Pelletier J, Housman D: The candidate Wilms' tumour gene is involved in genitourinary development. Nature 1990, 346:194–197
27. Devriendt K, Deloof E, Moerman P, Legius E, Vanhole C, de Zegher F, Proesmans W, Devlieger H: Diaphragmatic hernia in Denys-Drash syndrome. Am J Med Genet 1995, 57:97–101
28. Reardon W, Smith S, Suri M, Grant J, O'Neill D, Kelehan P, Fitzpatrick D, Hastie N: WT1 mutation is a cause of congenital diaphragmatic hernia associated with Meacham syndrome. American Society of Human Genetics (ASHG) 2004:802
29. Scott DA, Cooper ML, Stankiewicz P, Patel A, Potocki L, Cheung SW: Congenital diaphragmatic hernia in WAGR syndrome. Am J Med Genet A 2005, 134:430–433
30. White JC, Shankar VN, Highland M, Epstein ML, DeLuca HF, Clagett-Dame M: Defects in embryonic hindbrain development and fetal resorption resulting from vitamin A deficiency in the rat are prevented by feeding pharmacological levels of all-trans-retinoic acid. Proc Natl Acad Sci USA 1998, 95:13459–13464
31. Herzer U, Crocoll A, Barton D, Howells N, Englert C: The Wilms tumor suppressor gene wt1 is required for development of the spleen. Curr Biol 1999, 9:837–840
32. Angulo Y Gonzalez AW: The perinatal growth of the albino rat. Anat Rec 1932, 52:117–137
33. Greer JJ, Allan DW, Babiuk RP, Clugston R: Insights into the pathogenesis and etiology of congenital diaphragmatic hernia from rodent models. Fetal Matern Med Rev 2005, 16:211–220
34. Babiuk RP, Zhang W, Clugston R, Allan DW, Greer JJ: Embryological origins and development of the rat diaphragm. J Comp Neurol 2003, 455:477–487
35. Harrington SW: Various types of diaphragmatic hernia treated surgically: report of 430 cases. Surg Gynecol Obstet 1948, 86:735
36. Wells LJ: Development of the human diaphragm and pleural sacs. Carnegie Institution of Washington Publication 603, Contributions to Embryology 1954, 35:107–134
37. Ackerman KG, Herron BJ, Vargas SO, Huang H, Tevosian SG, Kochilas L, Rao C, Pober BR, Babiuk RP, Epstein JA, Greer JJ, Beier DR: Fog2 is required for normal diaphragm and lung development in mice and humans. PLoS Genet 2005, 1:e10
38. Yuan W, Rao Y, Babiuk RP, Greer JJ, Wu JY, Ornitz DM: A genetic model for a central (septum transversum) congenital diaphragmatic hernia in mice lacking Slit3. Proc Natl Acad Sci USA 2003, 100:5217–5222
39. Liu J, Zhang L, Wang D, Shen H, Jiang M, Mei P, Hayden PS, Sedor JR, Hu H: Congenital diaphragmatic hernia, kidney agenesis and cardiac defects associated with Slit3-deficiency in mice. Mech Dev 2003, 120:1059–1070
40. Biggio Jr JR, Descartes MD, Carroll AJ, Holt RL: Congenital diaphragmatic hernia: is 15q26.1-26.2 a candidate locus? Am J Med Genet A 2004, 126:183–185